Construction of an Atomic Beam System and Efficient Production of Metastable States

J.V.B. Gomide, G.A. Garcia, F.C. Cruz, A.J. Polaquini,
M.P. Arruda, D. Pereira, A. Scalabrin
Instituto de Física "Gleb Wataghin", Universidade Estadual de Campinas
UNICAMP, 13083-970, Campinas, SP, Brazil

Received January 23, 1997

We mounted a versatile atomic beam system, that can be operated with a large variety of chemical elements in their fundamental state or in metastable levels. This system permits to observe the electrical discharge region, turning possible to take the emission spectra of the excitation processes. The spectrum done for calcium is the first one in the literature in this condition, to our knowledge. After the excitation region, we found 45% of the atoms in the (4s4p) $^3P_{1,2,3}$ metastable triplet. In this work we present a general description of an atomic beam system, with the expected values for calcium and magnesium, and a detailed description of the vacuum system and the atomic source. We discuss the processes of excitation to the metastable levels, the characterization of the efficiency of the discharge to populate the metastable triplet and the emission spectra of the discharge region.

I. Introduction

This paper describes the construction of an atomic beam system and some initial measurements done to characterize the beam. The system is versatile, permitting the operation with several different chemical elements, in the ground state or in a mixture of fundamental and metastable states. We built the exit configuration of the oven with a geometry that permits to choose the type of beam to work.

The scope is to realize high resolution spectroscopy and laser manipulation of atoms in a beam, preparing the future construction of an atomic frequency standard (AFS). We are now working with calcium and, in the near future, with magnesium. The diagram level of the first excited states of these elements is shown in Fig. 1. Calcium has an important role in the theoretical and experimental development of atomic physics[1]. In the periodical table it is the first element before the fulfillment of the 3d orbital, presenting interesting results in orbital correlation[2]. The first photoelectronic spectrum using synchrotron radiation in a single ionized atom was done with calcium in an atomic beam[3]. Its nucleus has a magic number of protons and therefore various stables isotopes, with two of them (^{40}Ca and ^{48}Ca) presenting also magic number of neutrons, being of great interest for isotopic shift studies[4,5].

The magnetic dipole transitions of the metastable triplet ^{3}P fine structure are suitable for an AFS in the far infrared region of the spectrum, as proposed by Strumia[6], or in the visible, using the intercombination line $^1S_0$ - $^3P_1$ [7]. In the proposal of [6], the clock interrogation is between $^3P_0$ - $^3P_1$ or $^3P_2$ - $^3P_1$, respectively with 0.6 or 1.2 THz for Mg, and 1.6 or 3.2 THz for Ca. The signal is the Ramsey type fluorescence emitted in the intercombination line, caught some distance downstream by a photomultiplier.

A Mg AFS prototype in the 0.6 THz transition is now operating at the Istituto Elettrotenico "Galileo Ferraris", in Turin, with a short term stability of 10^{-12} in one second. Its experimental arrangement is shown in Fig. 2 [8]. Experiments of laser cooling and optical pumping are being done to improve the performance of the Mg AFS and to construct the Ca AFS[9-12].

We present in the next section a general description of an atomic beam system, with the expected values for calcium and magnesium, and a detailed description of the vacuum system and the atomic source. In section III the processes of excitation to the metastable lev-

els and the longitudinal electrical discharge used is discussed with the characterization of the efficiency of the discharge to populate the metastable triplet. Section IV has the emission spectra of the discharge region, the first reported in the literature to our knowledge, and we discuss the obtained results.

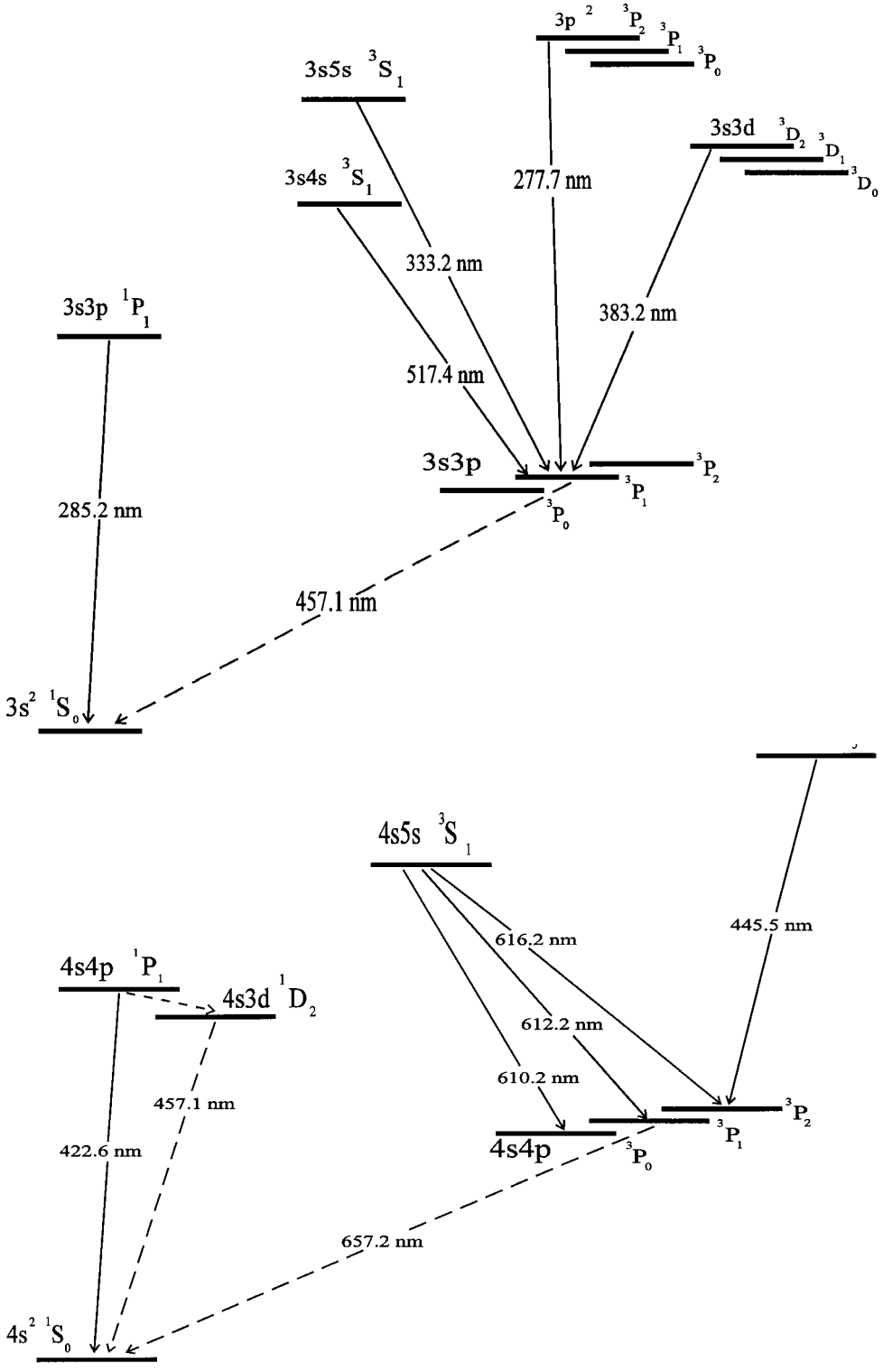

Figure 1. a) Diagram level of the first excited states of Magnesium; b) Transitions in the first excited states of Calcium.

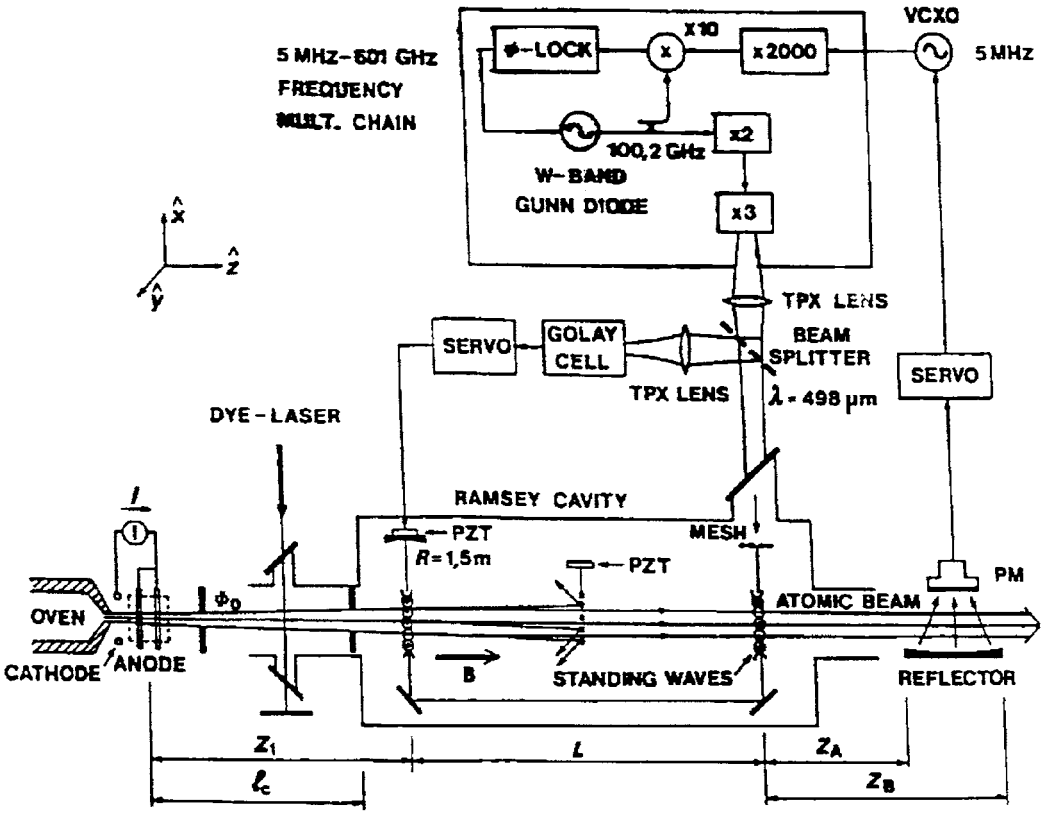

Figure 2. Experimental set-up of the Mg clock[8]. The distances are: $z_1 = 1.12$ m; $L = 0.3$ m; $z_B = 0.6$ m; $l_c = 0.97$ m.

II. Atomic beam system

II.1. General description

A typical atomic beam is constituted of a source of atoms and an evacuated medium where it passes, and it is described in various works, as the classic of N.F. Ramsey[13]. We designed the source of atoms to produce a well-defined beam of particles. The vacuum in the medium must be high enough to make the mean free path, λ_{MS}, much greater than the dimensions of the apparatus. The mean free path is given by

$$\lambda_{MS} = 7.3 \times 10^{-20} T/(P\sigma) \quad [\text{cm}] \qquad (1)$$

where σ the cross section for atomic collisions in cm^{-2}, T the absolute temperature and P the pressure in Torr[13]. In our case, the distance from the oven aperture until the window at the end of the atomic path is 116 cm. For high resolution spectroscopy purpose a pressure of 10^{-6} Torr is sufficient. In experiments of laser deceleration of atoms we have to work around 10^{-7} Torr, and with atomic molasses 10^{-9} Torr.

The atomic source of the system is a cylindrical oven with a 2 mm diameter and 3 mm lenght aperture, to allow the atoms to efuse from the source. To have effusion the mean free path of the atoms inside the oven must be greater or of the same magnitude of the dimension of the oven exit, that is, its diameter ($2r$) and its lenght (1). At the temperature of operation with calcium, 970 K, the mean free path is 0.9 mm, and with magnesium, 800 K, it is 1.5 mm. As a matter of fact, for most purposes sources are found effective when $2r \cong MS$, even for diameters slightly greater than λ_{MS} as in our case[13].

The total number of atoms per second that exit the oven, Q, is given by[13]

$$Q = (1/4k) n \langle v \rangle A_s \qquad (2)$$

where n is the atomic density inside the oven, $\langle v \rangle$ is the average velocity of the atoms in the oven, A_s is the area of the aperture ($A_s = 3.2$ mm^2), and $1/k$ is a factor that depends on the diameter and width of the aperture, equal to 0.9 in our case[13]. For calcium at 973 K, $n = 1.24 \times 10^{15}$ atoms/cm^3 [16], $\langle v \rangle = 717$ m/sec,

and $Q \sim 6.4 \times 10^{17}$ atoms/sec. For magnesium at 800 K, $n = 1.3 \times 10^{15}$ atoms/cm^3 [16], $\langle v \rangle = 831$ m/sec, and $Q \sim 7.8 \times 10^{17}$ atoms/sec.

II.2. vacuum system

In our atomic beam system, there are two vacuum chambers separated by a collimator with 2 mm diameter. Each chamber is evacuated by a turbomolecular pump with a flow rate of 240 1/s, each one connected to a double rotary vane mechanical pump. A view of the apparatus is shown in Fig. 3.

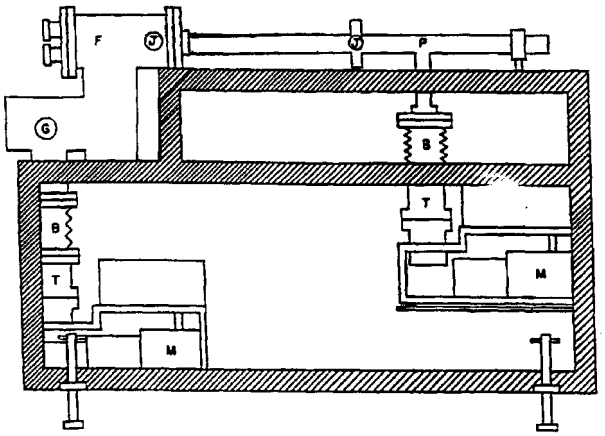

Figure 3. Atomic beam system constructed at Unicamp. F: oven region; J: window; G: Penning gauge head; P: pyrex tube; B: bellows; T: turbomolecular pump; M: double vane rotary pump.

The first chamber is a "T" shaped stainless steel construction, where is located the oven and, in one of the configurations, the electrical discharge. It has two side derivations with Pyrex windows, enabling direct observation of the oven exit. Because of this it was possible to observe the emission spectra in the discharge region. The "T" is connected through a bellow to the vacuum pump system. A Conflat flange closes the rear side of the T's upper arm. The oven is fixed in this flange, that also has two feedthroughs for the thermocouples and electrical signals. At the other side of the upper arm is another flange with the collimator, 11 cm apart from the oven exit, to reduce the divergence of the atomic beam. The second chamber is connected to the first one through this flange. It is basically a Pyrex tube with 5 cm diameter and 100 cm long, with Pyrex windows at its sides and end, giving access to the atomic beam to make high resolution spectroscopy and laser cooling. The tube is connected through a bellow to the other vacuum pump system.

The pressure is measured by two cold cathode gauge heads, one at the "T" and the other between the Pyrex tube and the turbomolecular pump, which permits to measure in the range from 10^{-3} to 10^{-10} Torr. A Pirani gauge head is placed between each turbomolecular and rotary pumps. Both sets of Penning-Pirani gauge heads send the signal to the pressure meter.

All the seals are of copper, with the exception of two Viton with centering ring seals at the Penning gauge heads. The final pressure of the system in this configuration is around 2×10^{-3} Torr, that increases to 2×10^{-7} when the oven is at the working temperature.

II.3. Atomic source

The source of atoms is basically a cylindrical oven designed for minimum heat loss to the exterior medium. The central structure is a stainless steel beaker (S), where we put the chemical element, surrounded by a copper wrapper, to permit a good thermal contact. The copper cover is surrounded by a coaxial resistor (H) that heats the oven. A schematic diagram of the atomic source with the electrical discharge is shown in Fig. 4.

A stainless-steel double-wall cylinder (D) coaxial to the central structure reduces the thermal radiation losses. The ensemble oven-double cylinder is supported by an external cylinder by means of screws that touch the oven in the minimum area possible. This external cylinder is fixed in the rear flange. In the configuration designed to excite the atomic beam, the electrical discharge is mounted at the top of this structure, as in Fig. 4.

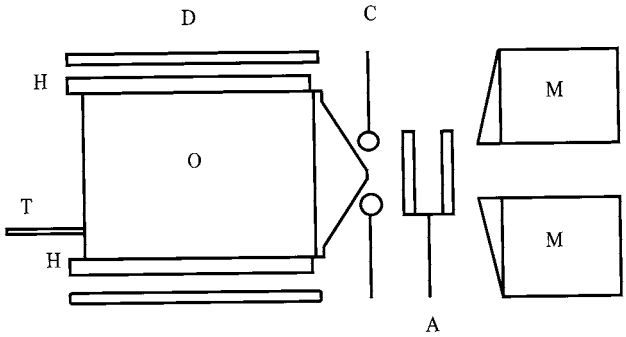

Figure 4. Schematic diagram of the oven with the electrical discharge. S: stainless steel beaker; H: resistance with the copper wrapper; D: double-wall cylinder; T: termocouple; C: cathode; A: double ring anode; M: magnet.

The coaxial resistor is fed by a thyristor power module. In the base of the oven is installed a K-type thermocouple. A PID temperature controller compares the

temperature set with the oven temperature and acts in the thyristor to send pulses of current to the resistor to approach the set point in a soft way, so that there is no significant fluctuation in the programmed temperature (less than 1 K).

The design of the oven exit changes with the type of atomic beam used. The exit temperature must be higher than the oven temperature itself, to avoid condensation of metal films in the aperture. The cathode heats the oven when we work with excited states and an additional resistor with another temperature controller is used when the beam is in the fundamental state, without the electrical discharge.

III. Efficient production of metastable states

III.1. Excitation processes

At the oven aperture almost all of the atoms are in the fundamental state. In fact, the relative population of the energy levels is given by the Boltzmann equation

$$N_j/N_i = (g_j/g_i)e^{-\Delta E/kT} \qquad (3)$$

where i and j are the initial and final states, respectively, N_j and N_j are the atom density, g_i and g_j the statistical weight of the states, k the Boltzmann constant, and T the absolute temperature. If j is referred to $^3P_1$ and i is the ground state, $N_j/N_i \sim 5 \times 10^{-10}$ for calcium and $N_j/N_i \sim 10^{-18}$ for magnesium.

Then it is necessary to intervene externally to populate the excited states. This can be done radiating the atomic beam with intense resonant light or bombarding the atoms in an electrical discharge. We choose the later because of the high efficiency of the electron-atom collisions to populate the excited states.

For the first metastable triplet of the alkaline-earth elements, the transitions from the fundamental state $^1S_0$ to $^3P_{0,1,2}$ are strongly forbidden, but because of a mixture of the wavefunctions of the sublevel $^3P_1$ and the singlet $^1P_1$, $^3P_1$ decays to the ground state with a lifetime of the order of milliseconds. The electrical discharge populates efficiently the metastable triplet, through direct excitation from the fundamental state or by cascade decay from the upper excited states. For all the alkaline-earth elements, departing from calcium, the energy of the first $^1D_2$ singlet is lower than the first $^1P_1$ singlet. It decays to the fundamental state by means of a electric quadrupole transition or by a spin forbidden decay to the $^3P_1$ and then to $^1S_0$, with a lifetime of 4.2 msec for Ca. Therefore in the calcium beam we have a mixture of atoms in the fundamental state $(4s^2)$ $^1S_0$ and metastable states (4s4p) $^3P_{0,1,2}$ and (4s3d) $^1D_2$.

The electrical discharge can be longitudinal or transversal to the atomic beam. As we are working with the metastable states without decelerating the atoms, the longitudinal configuration is chosen because it has a higher efficiency to populate them than the transversal one. The longitudinal discharge changes the velocity profile of the atoms in the beam[14].

III.2. The longitudinal electrical discharge

The electrical discharge is basically constituted by a cathode (C) and an anode (A) submitted to a magnetic field in the cathode-anode distance, as in Fig. 4. This structure is mounted on an iron disk that is fixed in the external stainless-steel cylinder of the oven. In this disk we put the electrical contacts for the cathode and anode and four rods which sustain the permanent magnet (M) that gives the magnetic field in the discharge region.

The cathode, made of tantalum wire wounded in a thoroidal form, is positioned near the oven aperture. It is coated by a high emissivity mixture of BaO and SrO, obtained from $BaCO_3$ and $SrCO_3$ through the reaction

$$BaCO_3 + \Delta E \rightarrow BaO + CO_2$$

$$SrCO_3 + \Delta E \rightarrow SrO + CO_2$$

This oxide mixture has a low extraction potential for the electrons (1 eV), while for tantalum it is of 10 eV. The cathode is heated by a current around 6 A, which represents a temperature around 1200 K in the cathode.

The anode is made of two tantalum rings separated from each other by 1 cm. An axial static magnetic field of the order of 300 G forces the electrons to describe funnel-like trajectories, increasing the atom-electron collision probability. The discharge works in two distinct regimes. In the regime before the rupture of the plasma formed between the electrodes, we have

a working point with 250 V and 50 mA, with the discharge working like a diode. Applying a potential difference of 1200 V with a capacitor bank, a self-sustained regime is stablished, with a working point of 35 V and 150 mA.

III.3. Production efficiency of the (4s4p) ^{3}P metastable triplet

To perform this measurement we used the (4s4p) $^3P_0$ - (4s5s) $^3S_1$ Ca transition, at 610.2 nm. The laser resonant with this transition is sent perpendicular to the atomic beam, 20 cm after the collimator. The radiation is obtained with a ring dye laser CR 699-21 working with Rhodamine 590, pumped by an argon ion laser Innova 200. We have measured the absorption of the laser by the atomic beam at the center of the transition.

We can make an evaluation of the absorber density at the line center when the population of (4s5s) $^3S_1$ is much lower than that of the (4s4p) $^3P_0$ and the line shape of the transition is Gaussian, with width $\Delta\nu$. In our case, from the geometry of the beam, we arrive to a Doppler linewidth transversal to the atomic beam of $\Delta\nu_D = 70$ Mhz, which is greater than the natural linewidth $\Delta\nu_n = 15$ MHz, and justifies the use of this aproach. Our measured value for this line is $\Delta\nu_D = 106$ Mhz as can be seen in Fig. 6. As is discussed in[15], the absorption coefficient κ_ν at the frequency ν is defined by the equation

$$I_\nu = I_0 \exp(-\kappa_\nu x) \tag{4}$$

where x is the thickness of the absorber and I_0 and I_v are the intensities of the incident and transmitted light, respectively. In the interaction region, $x = 1$ cm.

For a Doppler-broadened line of width $\Delta\nu_D$ the absorption can be expressed in terms of κ_0, the absorption coefficient at line center,

$$\kappa_0 = \frac{2}{\Delta\nu_D}\left(\frac{\ln 2}{\pi}\right)^{1/2}\frac{\lambda_0^2}{8\pi}\left(\frac{g_2}{g_1}\right)NA \tag{5}$$

where λ_0 is the absorption wavelength, g_2 and g_1 are the statistical weights of the upper and lower states, respectively, N is the (4s4p) $^3P_0$ level population and A is the upper state (4s5s) $^3S_1$ spontaneous transition probability. The lifetime of the (4s5s) $^3S_1$ level is $\tau = 10.7$ns [16] and $I_v/I_0 = 0.94$ at line center, with a cathode-anode electrical current of 200 mA. Then we found

$$N(^3P_0) = 1.7 \times 10^8 \text{ atoms/cm}^3 \tag{6}$$

Considering the relative populations of the metastable triplet, $^3P_0$: $^3P_1$: $^3P_2$ as 1: 3: 5, it is possible to determine the density of atoms in the $^3P_0$ state and the percentage of atoms in the metastable triplet. The atom density 31 cm after the discharge region is given by[13]

$$N = \frac{1}{4\pi}N_f\frac{A_c}{d^2} \tag{7}$$

where N_f is the atomic density in the oven, equal to 1.24×10^{15} atoms/cm^3 at 974 K, A_c is the collimator area and d the distance between the oven and the interaction region. Then, the atomic density at d is 3.3×10^9 atoms/cm^{3}6. In this way, we have around (45$\pm$10)% of the beam atoms in the metastable triplet. This efficiency value for the production of metastable triplets in Ca is of the same order of magnitude as that measured for Mg is a similar atomic beam apparatus[17]

IV. Emission spectra of the electrical discharge region

The system was constructed to permit detection of the light emitted in the discharge region, through a window distant 30 cm from it. To avoid deposition of calcium films in the window, we put an iron disk inside the vacuum chamber, in front of the window, that can be dislocated with a magnet to let the light pass when we are making the measurements.

The fluorescence from the discharge is focalized in the entrance slit of a double grating spectrometer SPEX 1402 and detected by a RCA C31034 photomultiplier. The signal from the photomultiplier is sent to a SR 570 low-noise current preamplifier and then to the computer.

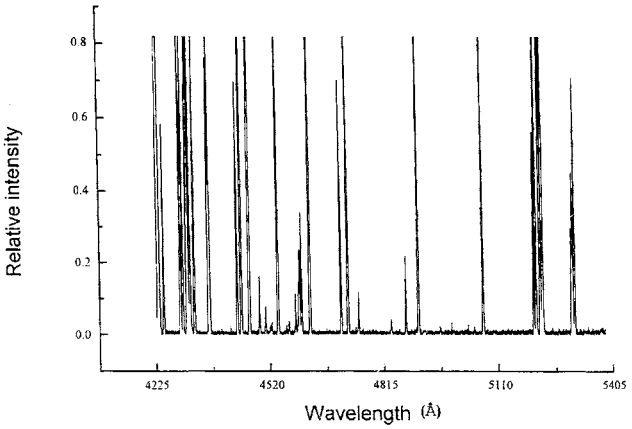

Figure 5. Spectrum obtained from the discharge region, between 4225 A and 5405 A.

Spectra from 3600 Å to 7340 Å were obtained during the pre-breakdown and self-sustained regimes of the discharge. In the pre-breakdown regime we observed almost only singlet transitions of low intensity, with the exception of the resonance line. When the discharge is in the self-sustained regime the intensities of the singlet transitions become orders of magnitude higher and then appear the lines of the triplet and single ionized transitions. In Fig. 5 we show the spectrum obtained between 4225 Å and 5405 Å. The more intense lines, with their relative intensities, are in the tables I, II and III, for the singlet, triplet and single ionized calcium, respectively. The intensity is given for the peak value, with the resonant transition $(4s^2)\ ^1S_0$ - (4s4p) $^1P_1$ equal to 1000.

We are doing calculations to identify the intensities of the fluorescence contributions from the various channels that populate the metastable states. With this we can determine the role developed by the direct excitation from the ground state or by the cascade decay from the higher excited levels to the metastable states.

From the data obtained, we observe that the intensities of the stronger lines of Ca II are comparable to that of the resonant line of Ca I. In fact, to obtain the self- sustained discharge condition by the atomic flux, the ion generation rate must garantee the charge conservation in the neutral region of the discharge. The intensity of the intercombination line $(4s^2)\ ^1S_0$ - (4s4p) $^3P_1$ is equal to 130.

The cascade decay from the higher levels is not taken into account in the theoretical models[14] and from the first experiments it seems to be very important in the population of the metastable triplet. To verify these hypothesis, it is necessary to change the parameters of the electrical discharge and look at the fluorescence intensities and the efficiency of production of metastable states. We have changed the data aquisition system to take spectra in lower time to achieve this scope.

λ (Å)	*Transition*	*Relative intensity*
3624.11-3645.00	$4p\ ^3P^0_{(0,1,2)}$-$5d\ ^3D_{(1,2,3)}$	70
4283.01-4318.65	$4p\ ^3P^0_{(0,1,2)}$-$4p^2\ ^3P_{(0,1,2)}$	410
4425.44-4456.61	$4p\ ^3P^0_{(0,1,2)}$-$4d\ ^3D_{(1,2,3)}$	510
4578.55-4585.96	$3d\ ^3D_{(1,2,3)}$-$4f\ ^3F^0_{(2,3,4)}$	100
5581.97-5602.85	$3d\ ^3D_{(1,2,3)}$-$4p\ ^3D^0_{(2,3,4)}$	370
6102.72-6162.17	$4p\ ^3P_{(0,1,2)}$-$5s\ ^3S_1$	370
6156.02-6169.56	$3d\ ^3D_{(1,2,3)}$-$5p\ ^3P^0_{(0,1,2)}$	200
6439.07-6508.85	$3d\ ^3D_{(1,2,3)}$-$4p'\ ^3F^0_{(2,3,4)}$	380

Table I: more intense triplet transitions of Ca I

λ (Å)	*Transition*	*Relative intensity*
4226.73	$4s^2\ ^1S_0$-$4p\ ^1P^0_1$	1000
4240.46	$3d\ ^1D_2$-$7p\ ^1P^0_1$	710
4355.08	$3d\ ^1D_2$-$5f\ ^1F^0_3$	220
4526.94	$3d\ ^1D_2$-$6p\ ^1P^0_1$	410
4685.27	$4p\ ^1P^0_0$-$6d\ ^1D_2$	210
4878.13	$3d\ ^1D_2$-$4f\ ^1F^0_3$	340
5041.62	$3d\ ^1D_2$-$4p'\ ^1P^0_1$	330
5188.85	$4p\ ^1P^0_0$-$5d\ ^1D_2$	440
5349.47	$3d\ ^1D_2$-$4f\ ^1F^0_3$	440
5512.98	$4p\ ^1P^0_0$-$4p^2\ ^1S_0$	170
5857.75	$4p\ ^1P^0_0$-$4p^2\ ^1D_2$	1000
5867.56	$4p\ ^1P^0_0$-$6s\ ^1S_0$	90
6717.69	$3d\ ^1D_2$-$5p\ ^1P^0_1$	410
7148.15	$3d\ ^1D_2$-$4p'\ ^1D^0_2$	300
7326.15	$4p\ ^1P^0_0$-$4d\ ^1D_2$	410

Table II: more intense singlet transitions of Ca I

λ (Å)	*Transition*	*Relative intensity*
3706.07	$4p\ ^2P_{1/2}$-$5s\ ^2S_{1/2}$	40
3736.90	$4p\ ^2P_{3/2}$-$5s\ ^2S_{1/2}$	100
3933.66	$4s\ ^2S_{1/2}$-$4p\ ^2P_{1/2}$	1000
3968.47	$4s\ ^2S_{1/2}$-$4p\ ^2P_{3/2}$	710

Table III: observed Ca II transitions

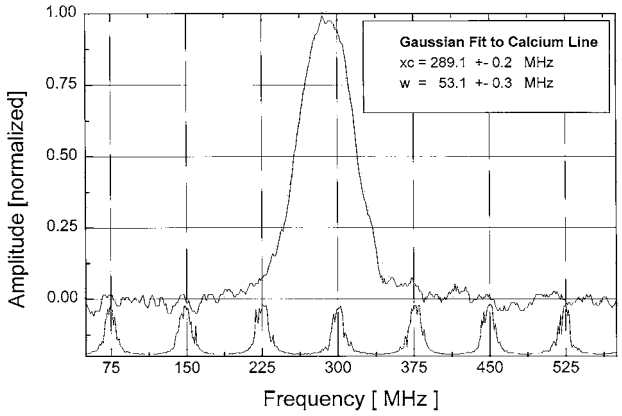

Figure 6. Optical pumping spectrum of the 610.2 nm Calcium line together with transmission peaks from a 75 MHz Fabry-Perot frequency marker. In the insert we can see data obtained from a gaussian fit of the line.

IV. Conclusions and perspectives

We have constructed with success, a versatile atomic beam system that permits operation with a large variety of atomic elements, in the fundamental state or in a mixture of fundamental and metastable states. We described the characteristics of this apparatus in general aspects and in our case using calcium and magnesium. The production efficiency of the triplet (4s4p) $^3P_{1,2,3}$ metastable state was determined by laser absorption.

The design of the system permits to observe directly the region around the oven exit. In this way, we took the emission spectra of the discharge region when we worked with calcium. These are the first spectra of calcium in these conditions reported in the literature, to our knowledge. It is possible, having the relative intensities and the wavelength of the transitions involved in the production of the metastable triplet, to carry out calculations to know the role of the various types of mechanisms that determine the population of the triplet. These calculations are being done and we believe that this will help to clarify the dynamics of production of these states, which is important to stabilish an Ca or Mg atomic frequency standard.

We improved the data aquisition to take the spectra from the discharge region in lower time. It will permite to detect the relative intensities of all the lines as we change the electrical discharge conditions. This will improve the experimental data that will be used to make the Multiconfiguration Hartree-Fock calculations.

In this moment we are measuring the velocity distribution of the metastable states to finalize the caracterization of the most important beam variables. Laser pumping of the ^3P states using the $^3P_{0,1,2}$ - $^3S_1$ transitions are also being done, with and without magnetic field, to determine the role of the σ and π transitions.

Otherwise, the applications of this atomic beam system are multiple, in high resolution atomic spectroscopy, involving lasers as well as other light sources, as syncrotron radiation, in atomic manipulation with light, or as an AFS.

Acknowledgements

We are grateful to Prof. F. Strumia, who gave us suggestions and passed us the know-how to construct this atomic beam system, and to Prof. N. Beverini, Dott. E. Maccioni and the technicians Mrs. M. Montanari and M. Francesconi, who gently helped us to construct some parts of the system, at Università di Pisa, Italy. We acknowledge P.A.P. Gomes and M.J. Ferreira at Laboratório Nacional de Luz Síncrotron (LNLS) who gave sugestions to construct the vacuum system and let us use the machines to make the stainless steel "T". Two of us (JVBG and GAG) received fellowships from Conselho Nacional de Desenvolvimento Científico e Tecnológico (CNPq) and Fundação de Amparo e Pesquisa do Estado de São Paulo (Fapesp) during the period of these experiments. This work was supported by Fapesp and CNPq.

References

1. J. Sugar and C. Corliss, J. Phys. Chem. Ref. Data **8**, 865 (1979).
2. N. Vaeck, M. Godefroid and J.E. Hansen, J. Phys. B **24**, 361 (1991).
3. 3. J.M. Bizeau, D. Cubaynes, E. Kallne, T.J. Morgan, J. Obert, J.-C. Putaux, M. Richter, S. Sorensen and F.J. Wuilleumier, Phys. Rev. Lett. **65**, 576 (1991).
4. A. Aspect, J. Bauche, M. Godefroid, P. Grangier, J.E. Hansen and N. Vaeck, J. Phys. B **24**, 4077 (1991).
5. W.H. King, *Isotope Shifts in Atomic Spectra*, Plenum Press, 1984.

6. F. Strumia, Metrologia **8,** 85 (1972); F. Strumia, in *Laser Science and Technology*, edited by A. N. Chester et al, Plenum Press, 367 (1988).
7. J. Helmcke, A. Morinaga, J. Ishikawa, F. Riehle, I.E.E.E Trans. IM-**38**, 524 (1989).
8. A. Godone and C. Novero, Metrologia **30**, 163 (1993).
9. For Mg cooling, see for example N. Beverini, S. De Pascalis, E. Maccioni, D. Pereira, F. Strumia, G. Vissani, Y.Z. Wang, C. Novero, Opt. Lett. **14**, 350 (1989); W.Q. Cai, N. Beverini, S. del Tredici, J.V.B. Gomide, E. Maccioni, and F. Strumia, SPIE Vol. 1726, p. 212, Shanghai, 1992; K. Sengstock, U. Sterr, G. Hennig, D. Bettermann, J.H. Muller, W. Ertmer, Opt. Commun. **103**, 73 (1993).
10. For Ca cooling, see for example N. Beverini, E. Maccioni, D. Pereira, F. Strumia, in Frequency Standards and Metrology, ed. A.De Marchi, Springer Verlag, pag. 282 (1989); T. Kurosu, F. Shimizu, Jap. Journ. Appl. Phys. **29**, 2127 (1990), N. Beverini, J.V.B. Gomide, E. Maccioni, F. Strumia, G. Vissani, in *Light Induced Kinetic Effects on Atoms, Ions and Molecules,* ed. L. Moi et al, ETS Editrice, p. 111 (1991); A. Witte, Th. Kisters, F. Riehle, J. Helmcke, J. Opt. Soc. Am. B-**9**, 1030 (1992).
11. For optical pumping in Mg, A. Godone, C. Novero, and E. Bava, IEEE Trans. Instrum. Meas. IM-**40**, 149 (1991); N. Beverini, W.Q. Cai, S. del Tredici, J.V.B. Gomide, E. Maccioni, A.M. Messina, F. Strumia, Opt. Commun. **110**, 309 (1994).
12. For pumping in Ca, J.V.B. Gomide, G.A. Garcia, F.C. Cruz, D. Pereira and A. Scalabrin, in International Quantum Electronics Conference Technical Digest, Anaheim, CA, USA, 1994.
13. N.F. Ramsey, **Molecular Beams**, Oxford Press, 1956 and 1985.
14. G. Giusfredi, A. Godone, E. Bava and C. Novero, J. Appl. Phys. **63**, 1279 (1988).
15. J. Tenenbaum, I. Smilanski, S. Gabay, G. Erez, and L.A. Levin, J. Appl. Phys. **49**, 2662 (1978).
16. Dushman, *Scientific Foundation of Vacuum Technology*, John Wiley and Sons, 2nd edition, 1966.
17. G. Giusfredi, A. Godone, E. Bava, C. Novero, J. Appl. Phys., **63** (5), 1279 (1988).
18. W. Gornik, D. Kaiser, W. Lange, J. Luther, K. Meier, H.-H Radloff and H. H. Shulz, Phys. Lett. **45A**, 219 (1973).